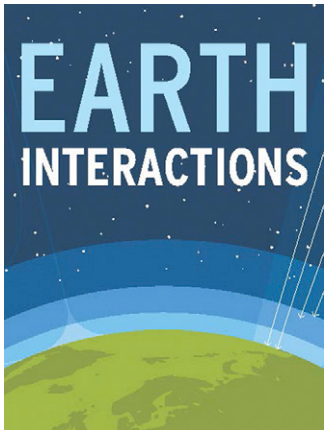

Does an Intrinsic Source Generate a Shared Low-Frequency Signature in Earth's Climate and Rotation Rate?

Steven L. Marcus*

Private Researcher, Santa Monica, California

Received 11 March 2015; in final form 24 October 2015

ABSTRACT: Previous studies have shown strong negative correlation between multidecadal signatures in length of day (LOD)—an inverse measure of Earth's rotational rate—and various climate indices. Mechanisms remain elusive. Climate processes are insufficient to explain observed rotational variability, leading many to hypothesize external (astronomical) forcing as a common source for observed low-frequency signatures. Here, an internal source, a core-to-climate, one-way chain of causality, is hypothesized. To test hypothesis feasibility, a recently published, model-estimated forced component is removed from an observed dataset of Northern Hemisphere (NH) surface temperatures to isolate the intrinsic component of climate variability, enhancing its comparison with LOD. To further explore the rotational connection to climate indices, the LOD anomaly record is compared with sea surface temperatures (SSTs)—global and regional. Because climate variability is most intensely expressed in the North Atlantic sector, LOD is compared to the dominant oceanic pattern there—the Atlantic multidecadal oscillation (AMO). Results reveal that the LOD-related

* Corresponding author address: Steven L. Marcus, 1133 Lincoln Blvd. #7, Santa Monica, CA 90403.

E-mail address: weatherp@gmail.com

DOI: 10.1175/EI-D-15-0014.1

signal is more global than regional, being greater in the global SST record than in the AMO or in global-mean (land + ocean) or land-only surface temperatures. Furthermore, the strong (4σ) correlation of LOD with the estimated NH intrinsic component is consistent with the view proffered here, one of an internally generated, core-to-climate process imprinted on both the climate and Earth's rotational rate. While the exact mechanism is not elucidated by this study's results, reported correlations of geomagnetic and volcanic activity with LOD offer prospects to explain observations in the context of a core-to-climate chain of causality.

KEYWORDS: Physical meteorology and climatology; Climate change; Temperature; Mathematical and statistical techniques; Time series; Variability; Multidecadal variability

1. Introduction

The origins of multidecadal oscillations in Earth's climate remain controversial (e.g., Solomon et al. 2010; Marcus et al. 2011; Kosaka and Xie 2013), with the North Atlantic region frequently emphasized as a potential pacesetter for their global propagation (e.g., Delworth and Mann 2000; Wyatt et al. 2012; Chen and Tung 2014). By contrast, multidecadal variability in Earth's rotation, in particular the fluctuations of a few milliseconds observed in the length of day (LOD), has been robustly attributed to torsional oscillations within the liquid outer core (e.g., Hide et al. 2000, henceforth HBD). Both of these oscillations have predominant periods in the 60–70-yr range (e.g., Schlesinger and Ramankutty 1994; Roberts et al. 2007, henceforth RYR), raising the possibility of their causal relation. Correlations between LOD and climate have long been reported; Lambeck and Cazenave (1976), in particular, found that negative LOD variations, corresponding to accelerations in Earth's rotation rate, tended to lead existing indices of ground pressure, global surface temperatures, and basin-scale atmospheric circulation patterns by about a decade. Noting, however, that the axial angular momentum associated with the circulation changes was an order of magnitude smaller than required to generate the concomitant variations of several milliseconds observed in LOD, they suggested that both the climate and LOD anomalies might have a common origin in solid Earth effects.

More recently, Dickey et al. (2011, henceforth DMV) used instrumental records of global-mean temperature extending back to the 1860s, corrected for anthropogenic effects by subtracting estimated forced changes computed from historical simulations made with coupled atmosphere–ocean general circulation models by two different groups, as a climate index for quantitative comparisons with LOD. They found significant correlations with (negative) LOD leading the model-corrected temperatures by 8 years, consistent with the paradigm that core oscillations may generate both decadal LOD changes through the instantaneous exchange of angular momentum with the overlying mantle and delayed surface temperature changes through as yet unspecified modifications to the surface and/or near-Earth environment (e.g., Usoskin et al. 2008).

Here, we pursue a two-pronged effort to confirm and extend these results: first, we use a more recent and comprehensive ensemble of energy balance and coupled model results, incorporating both natural and anthropogenic forcing (Mann et al. 2014, henceforth MSM) to correct Northern Hemisphere (NH) temperatures; and second, we compare the LOD data directly with regional [Atlantic multidecadal oscillation (AMO)] and global-mean sea surface temperatures (SSTs), as well as

global-mean surface and land surface temperatures, using only detrending on both data types to consistently eliminate the influence of secular processes, such as tidal braking and postglacial rebound, which are known to affect LOD on these time scales (e.g., Hide and Dickey 1991). The highly significant correlations obtained in both cases for temperature–LOD records extending back over two full cycles of the approximately 65-yr oscillation characterizing both data types (e.g., HBD; Wu et al. 2007) indicate that the processes that link them have been active during most of the period covered by global instrumental temperature records (Hansen and Lebedeff 1987) and robust LOD retrievals (Gross 2001).

The data types used and periods studied here are detailed in section 2, with results of the investigation presented in section 3. Section 4 provides a summary of our conclusions and a discussion of possible causal mechanisms linking core-generated changes in Earth rotation to multidecadal climate variability.

2. Data and methods

To isolate climate variations that may be related to Earth rotation, we use the semiempirical differenced approach of, for example, Schlesinger and Ramankutty (1994), Kravtsov and Spannagle (2008), DMV, and MSM, who subtracted model-computed temperatures from the observational record to recover variability not due to assumed known forcing mechanisms. MSM recently analyzed a comprehensive set of simulations from phase 5 of the Coupled Model Intercomparison Project (CMIP5) historical experiments (Stocker et al. 2013), deriving estimates of the forced (natural plus anthropogenic) component of NH mean temperature change by averaging over the full CMIP5 ensemble containing 163 realizations from 40 different models. These results were used to construct estimates of the unforced, internal variability of NH mean temperature (henceforth referred to as the ‘‘corrected’’ temperature) by subtracting them from observational records compiled by the Met Office Hadley Centre in collaboration with the Climatic Research Unit at the University of East Anglia (HadCRUT4; Brohan et al. 2006; Met Office 2015) beginning in 1850; comparisons were also made with the GISS Surface Temperature Analysis (GISTEMP; Hansen et al. 2006), beginning in 1880.

For purposes of comparison with the LOD data, we formed a single record of coupled model-corrected NH mean surface temperature by subtracting the MSM CMIP5 ensemble forcing estimate from the average of the HadCRUT4 and GISTEMP observational records, covering the period 1880–2005 common to all the data. MSM also used a zero-dimensional energy balance model (EBM) to estimate the response of NH temperature to radiative forcing, applying a best-fit methodology to parameterize anthropogenic aerosol, volcanic, and solar effects. We formed an EBM-corrected record of NH mean temperature for comparison with LOD by subtracting their optimized results from the averaged observational record over the same period.

To assess the potential relationship of LOD to AMO, a goal motivated by the strong presence of multidecadal variability, of the same tempo as LOD, centered in the North Atlantic, we also compared detrended but otherwise uncorrected SSTs with detrended LOD, using the global-mean series from HadSST3 (Kennedy et al. 2011; Climatic Research Unit 2014) and the regional AMO index from NOAA/Earth System Research Laboratory (Enfield et al. 2001) for the extended period 1872–2013; to place these results in context, HadCRUT4 (Brohan et al. 2006; Met

Office 2015) global mean (land + ocean) and Berkeley Earth project (Rohde et al. 2013; Berkeley Earth 2015) land-only surface temperatures were also compared with LOD over the same interval. The LOD series was taken from the LUNAR97 dataset beginning in 1832 (Gross 2001), with yearly averages of the daily COMB2012 dataset (Ratcliff and Gross 2013) appended to bring the record current; subtraction of yearly averaged effective atmospheric angular momentum values (Zhou et al. 2006; Atmospheric and Environmental Research 2014; not shown) from the COMB portion of the LOD record did not materially affect the results. All temperature series were first smoothed with a centered running mean of 5 years, thereby shortening the intervals over which the correlations were computed by 4 years.

Comparisons between the temperature and LOD data were performed using the Pearson correlation coefficient, computed as (e.g., Anderson 1958)

$$r = \frac{\sum_{i=1}^{n} (x_i - \overline{x})(y_i - \overline{y})}{\sqrt{\sum_{i=1}^{n} (x_i - \overline{x})^2} \sqrt{\sum_{i=1}^{n} (y_i - \overline{y})^2}}$$

for two series $X = [x_1, \ldots, x_n]$ and $Y = [y_1, \ldots, y_n]$.

To evaluate the significance of the correlation estimates, we adopt the null hypothesis that each detrended series represents an independent first-order autoregressive (AR1) process, for which the autocorrelation function (ACF) is

$$R(u) = \exp(-u/\tau),$$

where u is the lag, and τ is the decorrelation time for that process (e.g., Jenkins and Watts 1968). An estimate of τ, therefore, can be formed by determining the lag u_0, at which the sample ACF decreases to $1/e$. The number of degrees of freedom (DOF) for a given series segment is then taken to be the ratio of the length of the segment n to the estimated decorrelation time:

$$\mathrm{DOF} = n/u_0. \tag{1}$$

We employed the Fisher z transformation of the sample correlation coefficients (e.g., Anderson 1958),

$$z = \frac{1}{2} \log\left(\frac{1 + r}{1 - r}\right),$$

to obtain a statistic that is approximately normally distributed, with standard error

$$\sigma_z \approx \frac{1}{\sqrt{N - 3}},$$

where N is the number of independent observations in each of the correlated series. Since the temperature and LOD series used in this study have been smoothed (Gross 2001) and may contain long-period sources of variability (e.g., Delworth

and Mann 2000), we take the number of independent observations in each series N to be represented by its estimated DOF [Equation (1)]. Since z has a zero expected value under the null hypothesis of independent series, the number of standard deviations by which the sample value of z differs from zero,

$$s = z\sqrt{\mathrm{DOF} - 3}, \tag{2}$$

forms a measure of the significance of the obtained correlations, which we use here. To compute error estimates for the sample correlations (see Figure 2 below), the inverse of the Fisher z transformation $r_e = \tanh(z \pm \sigma_z)$ was used.

To compare the series with different statistical properties, the effective DOF is taken to be the geometric mean of the individual DOF for each [Equation (1)], decreased by one to account for the applied detrending. The lagged cross correlations were computed by keeping the temperature series fixed over the intervals defined above and comparing them with LOD series segments of equal length but sampled over earlier intervals corresponding to the lag being evaluated; autocorrelations for both data types were computed by comparing each detrended series with a lagged version of itself over the shorter interval common to both.

3. Results

The autocorrelation properties of the temperature and LOD series analyzed here, used to determine the effective DOF and hence the statistical significance of the cross correlations discussed below, are displayed in Figure 1. The decorrelation time for each series segment, used to compute the associated DOF [Equation (1)], is taken to be equal to the lag at which the corresponding autocorrelation decreases to $1/e$ (yellow shading in Figure 1), with linear interpolation between the yearly lagged estimates used to determine a precise value (third column in Table 1; logarithmic interpolation produces slightly shorter decorrelation times). Interestingly, the model-corrected NH temperatures (blue curves) are seen to have substantially shorter decorrelation times (denoted by red symbols) than the global and regional sea surface temperatures (green curves), leading to correspondingly higher DOF estimates (Table 1); land surface temperatures show an intermediate value. Autocorrelation estimates are also shown for the five leading, equal length segments of the LOD series (black curves) that are best correlated, respectively, with the temperature series listed in the caption (the cyan curves best correlate with LOD5). The LOD segment decorrelation times (denoted by magenta symbols) and hence the associated DOF are more nearly equal to each other (Table 1), so that the significance of the cross correlations will depend largely on the statistical properties of the temperature data employed.

All cross correlations (Figure 2) were calculated using the negative of the LOD index, corresponding to positive anomalies in Earth's rotational speed of a few parts in 10^8, leading the temperature series by the number of years indicated on the lower axis; the maximum correlation for each series and the corresponding standard (1σ) error bars are highlighted in red. Interestingly, the highest correlation ($r = 0.83$), with the (negative) LOD leading by 6 years, is obtained for the global SST. Both the SST and LOD series (Figure 3, bottom center panel) display strong variability on 60–70-yr time scales, as found in previous studies of core/LOD oscillations (HBD; RYR)

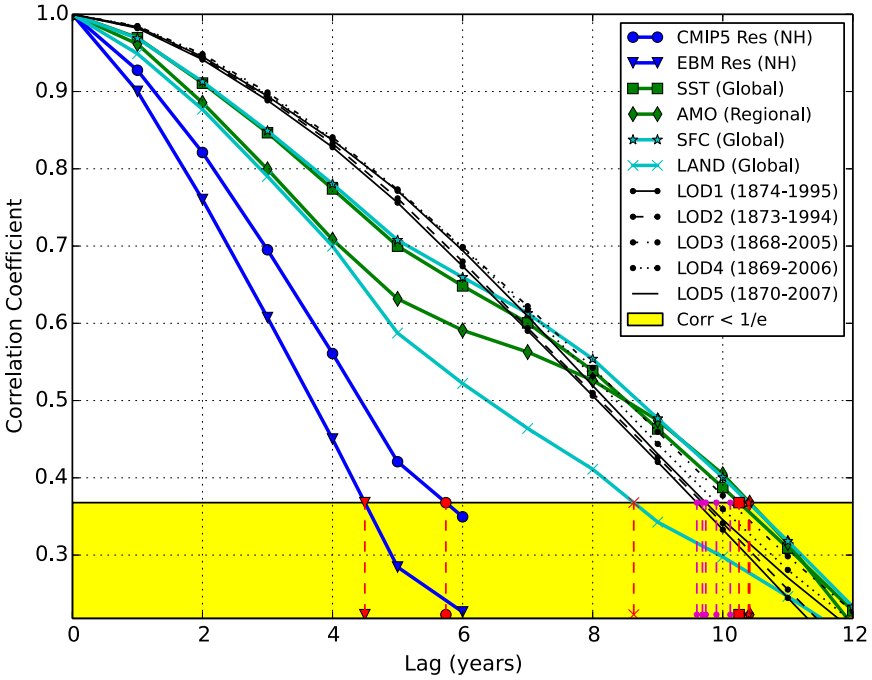

Figure 1. Autocorrelation properties for NH model–corrected (blue), global and regional sea surface (green), and global-mean (land + ocean) and land-only (cyan) surface temperature series (first smoothed with 5-yr running means) and for the equal length LOD series segments (black) with which each is respectively best correlated (the cyan curves best correlate with LOD5), after detrending over the intervals listed in Table 1. The yellow shading indicates where the autocorrelation for each temperature series or LOD series segment falls below 1/*e*, with the red (magenta) symbols and vertical dashed lines showing the linearly interpolated decorrelation times, marked on the lower axis, for the temperature (LOD) data (numerical values listed in Table 1).

and global temperature variability (e.g., Wu et al. 2011). The computed z value for the maximum correlation differs from zero by 3.67 standard deviations (Table 1), making it highly significant relative to a null hypothesis of independent AR1 processes for the SST and LOD series. Global mean (land + ocean; Brohan et al. 2006; Met Office 2015) and land-only (Rohde et al. 2013; Berkeley Earth 2015) surface temperatures (Figure 3, left panels) correlate at successively lower levels ($r = 0.74$ and $r = 0.50$) and a shorter lag (4 yr) with (negative) LOD, implying a rotational response weaker and more rapid for land than ocean surfaces.

Similar treatment of the next highest cross-correlation maximum ($r = 0.82$), obtained for the CMIP5-corrected NH temperatures lagging the (negative) LOD by 8 years over the slightly shorter 122-yr span shown in Figure 3 (bottom right panel), gives a z value differing from zero by over four standard deviations (Table 1), the most significant obtained in this study. To confirm the robustness of this result we generated 1000 realizations of an AR1 process having the same length as the CMIP5-corrected NH temperature series, according to

Table 1. Statistical properties of the temperature and LOD data used in this study. Rows 1–2 refer to model-corrected Northern Hemisphere temperatures, rows 3–4 refer to detrended but otherwise uncorrected global (GL) and regional (RG; Atlantic multidecadal oscillation) sea surface temperatures, rows 5–6 refer to global-mean (land + ocean) and land-only surface temperatures, and rows 7–11 refer to the equal length LOD series segments that best correlate, respectively, with each of the temperature series (LOD5 best correlates with both SFC and LND). Lengths of the series are given in column 2, decorrelation times are given in column 3, and the resulting degrees of freedom are given in column 4. The maximum (negative) LOD correlation for each temperature series is given in column 5, the LOD lead for each maximum correlation is given in column 6, and the number of standard deviations by which each maximum correlation differs from zero, using the Fisher z transformation statistic (Equation (2)), is given in column 7; the highest correlation and significance values are highlighted in italic and bold fonts in columns 5 and 7, respectively.

Data series	Length (yr)	Decorrelation (yr)	DOF (quotient)	LOD (negative) correlation	LOD lead (yr)	Fisher z std dev
NH-CMIP5	122	5.74	21.2	0.82	8	**4.07**
NH-EBM	122	4.50	27.1	0.63	9	2.82
SST (GL)	138	10.25	13.5	*0.83*	6	3.67
AMO (RG)	138	10.44	13.2	0.74	5	2.94
SFC (GL)	138	10.40	13.3	0.74	4	2.97
LND (GL)	138	8.63	16.0	0.50	4	1.83
LOD1	122	9.60	12.7	—	—	—
LOD2	122	9.69	12.6	—	—	—
LOD3	138	10.12	13.6	—	—	—
LOD4	138	9.90	13.9	—	—	—
LOD5	138	9.74	14.2			

$$x_{n+1} = \alpha x_n + w,$$

where w represents a random normal variable with zero mean and unit variance. For a value of $\alpha = 0.85$, the 5-yr smoothed, detrended realizations had a mean decorrelation time nearly equal to that observed for the similarly smoothed and detrended CMIP5-corrected NH temperatures (Figure 4, upper panel). The lower panel, however, shows that the correlation obtained for the observed temperature residual, with (negative) LOD leading by 8 years, exceeded the maximum absolute correlation obtained for any of the AR1 realizations, with equal length segments of the LOD series leading the observed NH temperatures by intervals of 0–16 years. Note, in particular, the wide disparity between the observed and the mean of the AR1 correlations with LOD (red and blue bars), confirming the significance of the former with respect to a null hypothesis of uncorrelated AR1 processes for the LOD and temperature series.

In addition to its higher level of significance, the CMIP5-corrected NH temperature correlation also shows a sharper maximum as a function of LOD lead time than is obtained for the uncorrected temperatures (Figure 2), confirming the 8-yr LOD lead found by DMV using a smaller ensemble of anthropogenically forced simulations to correct global-mean surface temperatures. The maximum correlation ($r = 0.63$) of EBM-corrected NH temperature (Figure 3, upper-right panel) with LOD also occurs at a lag of nearly a decade (Table 1), thereby helping to

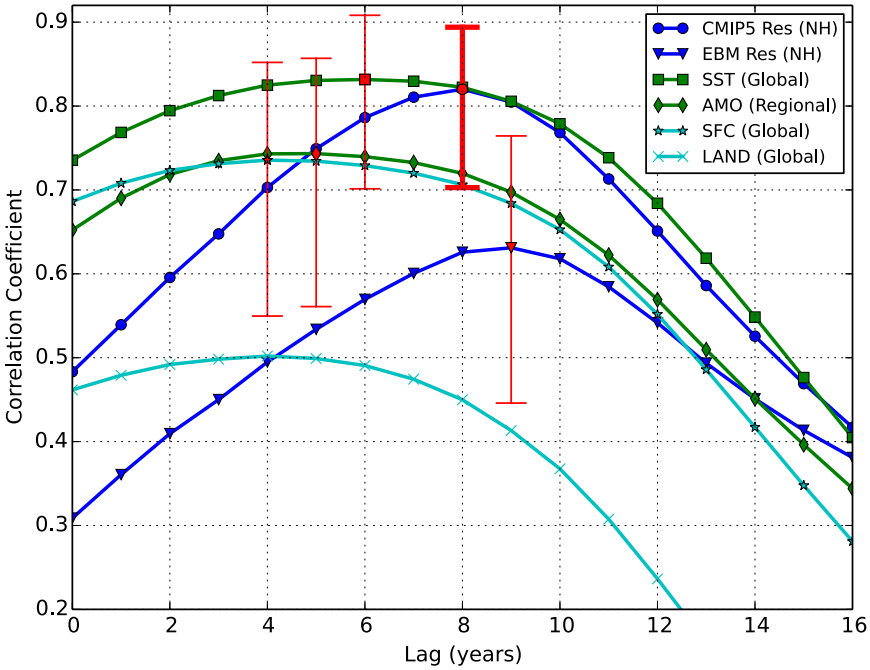

Figure 2. Correlations for NH model–corrected (blue), global and regional sea surface (green), and global-mean (land + ocean) and land-only (cyan) surface temperature series lagging (negative) LOD by the time indicated on the lower axis; standard error bars (red) are shown (in bold) for maximum correlations that are significant at or above the 2σ (4σ) level. Temperatures were first detrended over the intervals listed in Table 1 and smoothed with 5-yr running means.

establish the robustness of the model-corrected temperature–LOD phasing (blue curves in Figure 2). The regional AMO index (Figure 3, upper center panel) displays a less well-defined correlation maximum with LOD at a lag of 5 years (Figure 2); its substantially lower amplitude ($r = 0.74$) and significance level, compared to those obtained for the global SST maximum correlation (Table 1), argue against a central role for the AMO—as defined by the annual, area-averaged SST over the North Atlantic (Enfield et al. 2001)—in the multidecadal LOD–climate link studied here.

4. Summary and discussion

We investigated the correlations of two types of temperature records with LOD: NH mean surface temperatures corrected by CMIP5 and EBM simulations, using both natural and anthropogenic forcing; and detrended, but otherwise uncorrected, global mean and regional (AMO) sea surface temperatures (SSTs), with global mean (land + ocean) and land-only surface temperatures also considered. The highest correlation ($r = 0.83$) was found for the uncorrected global SST, with the (negative) LOD leading by 6 years (Figure 3, lower center panel). As noted by DMV, changes in ocean angular momentum due to plausible decadal current and

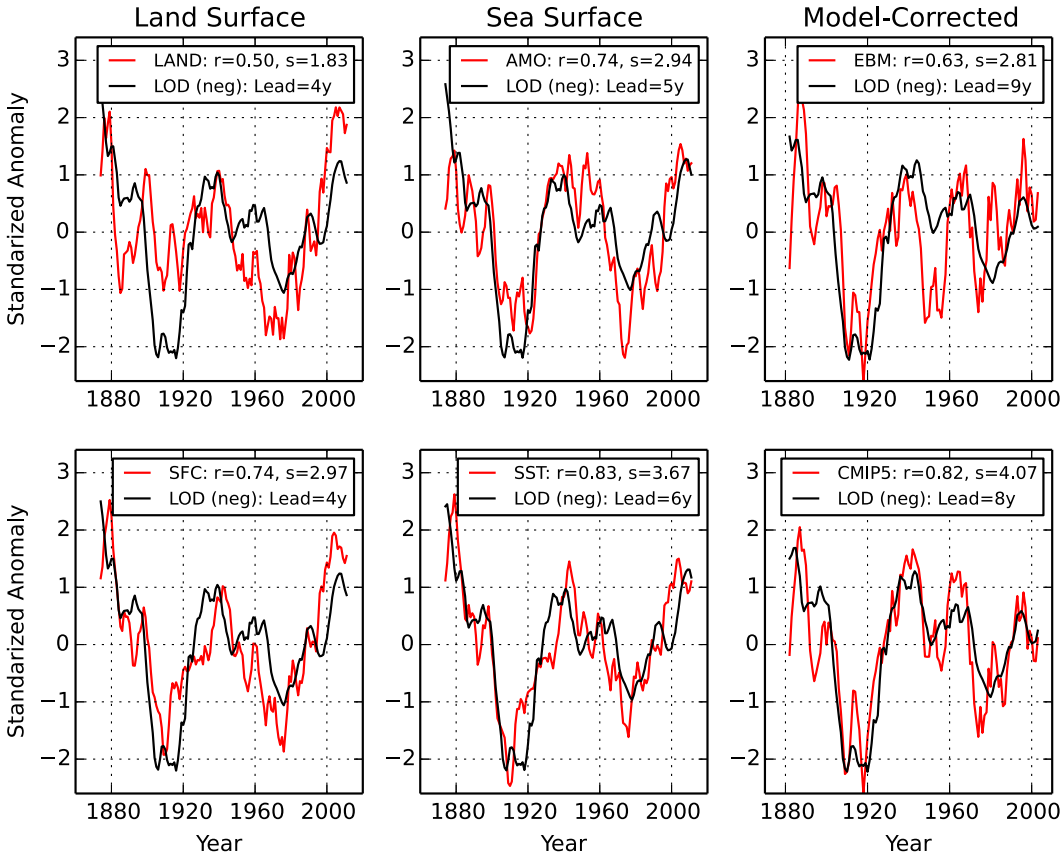

Figure 3. Comparison of temperature series (red) and the leading LOD series segment (black) with which each is best correlated; all series have been detrended and normalized to unit variance over the intervals shown. (left) Global-mean temperatures for (top) land-only and (bottom) land + ocean surfaces. (center) Sea surface temperatures for the North Atlantic in the top and global mean in the bottom. (right) Model-corrected NH temperatures, using (top) EBM and (bottom) CMIP5 estimates to remove known natural and anthropogenic forcing effects. The correlation coefficient and number of standard deviations by which it deviates from zero are shown by the *r* and *s* parameters, respectively, in each panel.

mass redistributions are too small to generate the concomitant, several millisecond variations observed in LOD. A reverse effect—for example, SST anomalies arising from vertical mixing or internal wave activity driven by rotational changes—would be difficult to detect in the presence of larger sources of oceanic dissipation (the appendix; see also Lambeck and Cazenave 1976), rendering a dynamical explanation for the large SST–LOD correlation noted here unlikely.

While the highest magnitude correlation was found with global SST, the highest level of significance [$s = 4.07$; cf. Equation (2)] was obtained for a similarly strong correlation ($r = 0.82$) with CMIP5-corrected NH temperatures lagging (negative) LOD by 8 years (Figure 3, lower-right panel). RYR detected significant multidecadal variability in the orientation of the geomagnetic field at the same lag with

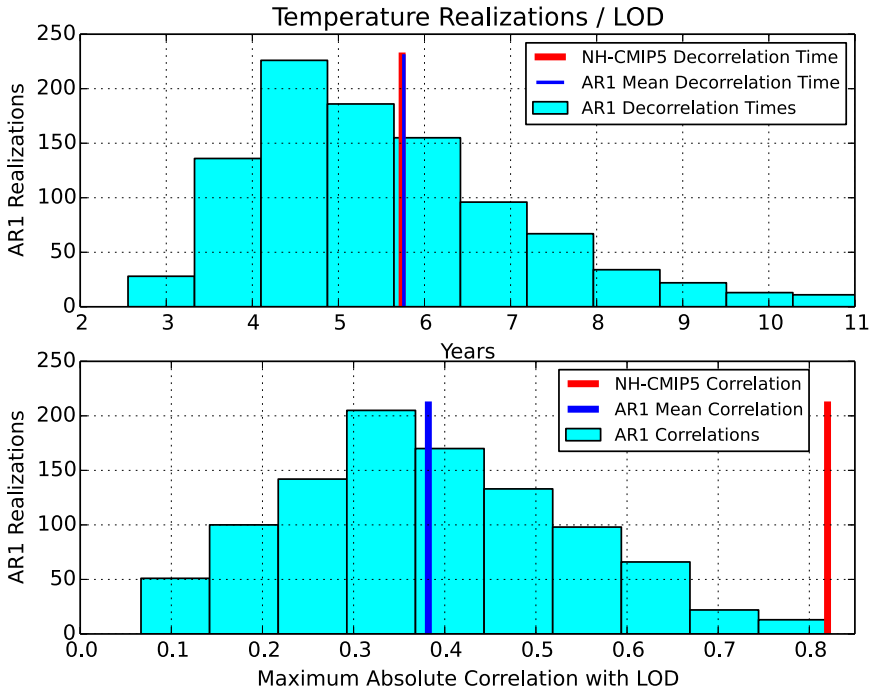

Figure 4. Statistical properties for 1000 AR1 series (cyan bars; see text) with the same length as the CMIP5-corrected NH temperature series (NH-CMIP5). (top) Decorrelation times for the 5-yr smoothed, detrended series; note the near equality of the NH-CMIP5 value (red bar) and the AR1 mean (blue bar; AR1 values > 11 years not shown). (bottom) Maximum absolute correlations obtained with LOD series segments leading the NH-CMIP5 temperatures by intervals of 0–16 years; note the wide disparity between the NH-CMIP5 value and the AR1 mean.

respect to LOD, while Kerton (2009) argued that the position of the magnetic poles—where the horizontal (shielding) component of the terrestrial field vanishes—relative to climatically sensitive areas such as the Arctic and North Atlantic Oceans might influence the pronounced multidecadal variability that originates there (e.g., Yeager and Danabasoglu 2014). Wyatt and Curry (2014) reported significant LOD correlations with Arctic climate indices over the twentieth century, and we found a strong correlation for the Atlantic multidecadal oscillation (AMO) regional SST with LOD; however, the larger magnitude and significance level obtained for the LOD correlation with global SST (Table 1) argues against a direct interaction between core-induced LOD, the orientation of the geomagnetic field, and the AMO. The synchronous geomagnetic and model-corrected NH temperature phasing with respect to LOD, nonetheless, leaves open the possibility of a global-scale connection between magnetic and climatic processes (e.g., Courtillot et al. 2007). The correlation reported by Mazzarella and Scafetta (2012) between global SST, negative LOD, and an index of NH auroral frequency is consistent with this hypothesis, although our interpretation would place the origin of these phenomena in core oscillations of the type described by HBD, rather than

the astronomical sources they invoked; further discussion on possible, external sources of shared LOD–climate variability is provided by Sidorenkov (2005).

An intriguing possibility for the LOD–climate connection is raised by Palladino and Sottili (2014), who find a significant correlation between changing LOD and the level of global volcanic activity, which may have a detectable signature in multidecadal climate variability (e.g., Ottera et al. 2010). Although volcanic forcing was accounted for in both the EBM and CMIP5 NH simulations considered here, imperfect removal of their effects could leave a detectable signal in the residual temperature series, particularly if other forcing agents, such as anthropogenic effects, are more accurately modeled. If similar mechanisms connect rotational variability to submarine volcanic and/or geothermal fluxes, which appear susceptible to small changes in tidal/orbital forcing (Tolstoy 2015) and may impact deep-water formation rates (Hofmann and Morales Maqueda 2009) or Ekman-induced heat transport (Pratt 2014), this provides another potential pathway for the LOD–climate link and in particular for its maximum expression in the global SST index.

In view of the substantially lower LOD correlations for temperatures incorporating land surfaces (section 3), the higher significance and nearly equal correlation levels obtained for the CMIP5-corrected NH mean (land + ocean) surface temperatures, compared to those for global SST (Table 1), attest to the efficacy of the correction procedure used (section 2) to isolate the internal NH temperature component for comparison with LOD, notwithstanding potential caveats regarding the fidelity of the coupled model results raised by Kravtsov et al. (2014) and Steinman et al. (2015). Thus, while a regional connection to negative LOD variability through the AMO (as conventionally defined) is not supported by our results, connections to both the observed detrended global SST and the CMIP5-corrected NH land + ocean temperatures are supported. Whether the physical mechanism(s) responsible for this link operate through dynamic, geomagnetic, volcanic/geothermal, or other intrinsic effects, our study suggests that the most likely source of the highly significant LOD correlations obtained for this pair of datasets—one containing only SSTs (global), while the other includes both SSTs and land surface temperatures (hemispheric)—lies in a nonnegligible contribution to multidecadal climate variability via core-induced rotational and/or related global-scale processes and hence to observed nonlinear trend changes in the rate of anthropogenic warming.

Acknowledgments. The author thanks Richard Gross and Michael Mann, respectively, for making available the length-of-day and modeled temperature data used in this study, and the Hadley Centre, Climate Research Unit, Goddard Institute for Space Studies, and the Berkeley Earth project for making available the observed temperature data. Comments from two anonymous reviewers helped to improve the clarity and focus of the manuscript.

APPENDIX

Rotational Kinetic Energy Change of the Ocean

For an ocean rotating with angular velocity

$$\Omega_0 = 2\pi/\mathrm{LOD}_0 \equiv 2\pi/86400\ \mathrm{s}^{-1}$$

and axial moment of inertia fixed at

$$I_{zz} \approx 4 \times 10^{34}\,\mathrm{kg\,m^2},$$

the kinetic energy of rotation is

$$K_0 = \frac{1}{2} I_{zz} \Omega_0^2 \approx 10^{26}\,\mathrm{J},$$

and a perturbation with

$$\Delta\Omega/\Omega_0 \approx -\Delta\mathrm{LOD}/\mathrm{LOD}_0$$

yields a kinetic energy change of amplitude

$$\Delta K \approx I_{zz}\Omega_0 \Delta\Omega \approx I_{zz}\Omega_0^2 \frac{\Delta\mathrm{LOD}}{\mathrm{LOD}_0} = 2K_0 \frac{\Delta\mathrm{LOD}}{\mathrm{LOD}_0}.$$

A decadal ($\tau = 10\,\mathrm{yr}$) variation of $\Delta\mathrm{LOD} \sim 3\,\mathrm{ms}$, for example, yields an average power

$$\Delta K/\tau \approx 22\,\mathrm{GW},$$

some two orders of magnitude less than the estimated oceanic dissipation rate of 2 TW (Hofmann and Morales Maqueda 2009).

References

Anderson, T. W., 1958: *An Introduction to Multivariate Statistical Analysis*. Wiley, 374 pp.

Atmospheric and Environmental Research, 2014: Special Bureau for the Atmosphere: Effective atmospheric angular momentum. Atmospheric and Environmental Research, accessed 22 September 2014. [Available online at ftp.aer.com/pub/anon_collaborations/AU5sba/aamf.ncep.reanalysis.1948.2014.]

Berkeley Earth, 2015: Global five-year mean land surface temperature. Estimated global land-surface TAVG based on the complete Berkeley dataset, Berkeley Earth, accessed 18 August 2015. [Available online at http://berkeleyearth.lbl.gov/auto/Global/Complete_TAVG_complete.txt.]

Brohan, P., J. J. Kennedy, I. Harris, S. F. B. Tett, and P. D. Jones, 2006: Uncertainty estimates in regional and global observed temperature changes: A new data set from 1850. *J. Geophys. Res.*, **111**, D12106, doi:10.1029/2005JD006548.

Chen, X., and K. K. Tung, 2014: Varying planetary heat sink led to global-warming slowdown and acceleration. *Science*, **345**, 897–903, doi:10.1126/science.1254937.

Climatic Research Unit, 2014: Global SST series. Climatic Research Unit, University of East Anglia, accessed 22 September 2014. [Available online at http://www.cru.uea.ac.uk/cru/data/temperature/HadSST3-gl.dat.]

Courtillot, V., Y. Gallet, J.-L. Le Mouel, F. Fluteau, and A. Genevey, 2007: Are there connections between the Earth's magnetic field and climate? *Earth Planet. Sci. Lett.*, **253**, 328–339, doi:10.1016/j.epsl.2006.10.032.

Delworth, T. L., and M. E. Mann, 2000: Observed and simulated multidecadal variability in the Northern Hemisphere. *Climate Dyn.*, **16**, 661–676, doi:10.1007/s003820000075.

Dickey, J. O., S. L. Marcus, and O. de Viron, 2011: Air temperature and anthropogenic forcing: Insights from the solid Earth. *J. Climate*, **24**, 569–574, doi:10.1175/2010JCLI3500.1.

Enfield, D. B., A. M. Mestas-Nunez, and P. J. Trimble, 2001: The Atlantic multidecadal oscillation and its relation to rainfall and river flows in the continental U.S. *Geophys. Res. Lett.*, **28**, 2077–2080, doi:10.1029/2000GL012745.

Gross, R. S., 2001: A combined length-of-day series spanning 1832–1997: LUNAR97. *Phys. Earth Planet. Inter.*, **123**, 65–76, doi:10.1016/S0031-9201(00)00217-X.

Hansen, J., and S. Lebedeff, 1987: Global trends of measured surface air temperature. *J. Geophys. Res.*, **92**, 13 345–13 372, doi:10.1029/JD092iD11p13345.

——, M. Sato, R. Ruedy, K. Lo, D. W. Lea, and M. Medina-Elizade, 2006: Global temperature change. *Proc. Natl. Acad. Sci. USA*, **103**, 14 288–14 293, doi:10.1073/pnas.0606291103.

Hide, R., and J. O. Dickey, 1991: Earth's variable rotation. *Science*, **253**, 629–637, doi:10.1126/science.253.5020.629.

——, D. H. Boggs, and J. O. Dickey, 2000: Angular momentum fluctuations within the Earth's liquid core and torsional oscillations of the core–mantle system. *Geophys. J. Int.*, **143**, 777–786, doi:10.1046/j.0956-540X.2000.01283.x.

Hofmann, M., and M. A. Morales Maqueda, 2009: Geothermal heat flux and its influence on the oceanic abyssal circulation and radiocarbon distribution. *Geophys. Res. Lett.*, **36**, L03603, doi:10.1029/2008GL036078.

Jenkins, G. M., and D. G. Watts, 1968: *Spectral Analysis and Its Applications*. Holden-Day, 525 pp.

Kennedy, J. J., N. A. Rayner, R. O. Smith, D. E. Parker, and M. Saundy, 2011: Reassessing biases and other uncertainties in sea surface temperature observations measured in situ since 1850: 2. Biases and homogenization. *J. Geophys. Res.*, **116**, D14104, doi:10.1029/2010JD015220.

Kerton, A. K., 2009: Climate change and the Earth's magnetic poles, a possible connection. *Energy Environ.*, **20**, 75–83, doi:10.1260/095830509787689286.

Kosaka, Y., and S. P. Xie, 2013: Recent global-warming hiatus tied to equatorial Pacific surface cooling. *Nature*, **501**, 403–407, doi:10.1038/nature12534.

Kravtsov, S., and C. Spannagle, 2008: Multidecadal climate variability in observed and modeled surface temperatures. *J. Climate*, **21**, 1104–1121, doi:10.1175/2007JCLI1874.1.

——, M. G. Wyatt, J. A. Curry, and A. A. Tsonis, 2014: Two contrasting views of multidecadal climate variability in the twentieth century. *Geophys. Res. Lett.*, **41**, 6881–6888, doi:10.1002/2014GL061416.

Lambeck, K., and A. Cazenave, 1976: Long term variations in the length of day and climatic change. *Geophys. J. Int.*, **46**, 555–573, doi:10.1111/j.1365-246X.1976.tb01248.x.

Mann, M. E., B. A. Steinman, and S. K. Miller, 2014: On forced temperature changes, internal variability, and the AMO. *Geophys. Res. Lett.*, **41**, 3211–3219, doi:10.1002/2014GL059233.

Marcus, S. L., O. de Viron, and J. O. Dickey, 2011: Abrupt atmospheric torque changes and their role in the 1976–1977 climate regime shift. *J. Geophys. Res.*, **116**, D03107, doi:10.1029/2010JD015032.

Mazzarella, A., and N. Scafetta, 2012: Evidences for a quasi 60-year North Atlantic Oscillation since 1700 and its meaning for global climate changes. *Theor. Appl. Climatol.*, **107**, 599–609, doi:10.1007/s00704-011-0499-4.

Met Office, 2015: Met Office Hadley Centre observations datasets. Met Office, accessed 18 August 2015. [Available online at http://www.metoffice.gov.uk/hadobs/hadcrut4/data/current/download.html.]

Ottera, O. H., M. Bentsen, H. Drange, and L. Suo, 2010: External forcing as a metronome for Atlantic multidecadal variability. *Nat. Geosci.*, **3**, 688–694, doi:10.1038/ngeo955.

Palladino, D. M., and G. Sottili, 2014: Earth's spin and volcanic eruptions: Evidence for mutual cause-and-effect interactions? *Terra Nova*, **26**, 78–84, doi:10.1111/ter.12073.

Pratt, V. R., 2014: An Ekman transport mechanism for the Atlantic multidecadal oscillation. *2014 Fall Meeting*, San Francisco, CA, Amer. Geophys. Union, Abstract GC21C-0566.

Ratcliff, J. T., and R. S. Gross, 2013: Combinations of Earth orientation measurements: SPACE2012, COMB2012, and POLE2012. Jet Propulsion Laboratory Tech Rep. JPL Publications 13-16, 30 pp. [Available online at http://ntrs.nasa.gov/archive/nasa/casi.ntrs.nasa.gov/20140011392.pdf.]

Roberts, P. H., Z. J. Yu, and C. T. Russell, 2007: On the 60-year signal from the core. *Geophys. Astrophys. Fluid Dyn.*, **101**, 11–35, doi:10.1080/03091920601083820.

Rohde, R., and Coauthors, 2013: A new estimate of the average Earth surface land temperature spanning 1753 to 2011. *Geoinfor. Geostat: Overview*, **1**, doi:10.4172/2327-4581.1000101.

Schlesinger, M. E., and N. Ramankutty, 1994: An oscillation in the global climate system of period 65–70 years. *Nature*, **367**, 723–726, doi:10.1038/367723a0.

Sidorenkov, N. S., 2005: Physics of the Earth's rotation instabilities. *Astron. Astrophys. Trans.*, **24**, 425–439, doi:10.1080/10556790600593506.

Solomon, S., K. H. Rosenlof, R. W. Portmann, J. S. Daniel, S. M. Davis, T. J. Stanford, and G.-K. Plattner, 2010: Contributions of stratospheric water vapor to decadal changes in the rate of global warming. *Science*, **327**, 1219–1223, doi:10.1126/science.1182488.

Steinman, B. A., M. E. Mann, and S. K. Miller, 2015: Atlantic and Pacific multidecadal oscillations and Northern Hemisphere temperatures. *Science*, **347**, 988–991, doi:10.1126/science.1257856.

Stocker, T. F., and Coauthors, 2013: Technical summary. *Climate Change 2013: The Physical Science Basis*, T. F. Stocker et al., Eds., Cambridge University Press, 33–115.

Tolstoy, M., 2015: Mid-ocean ridge eruptions as a climate valve. *Geophys. Res. Lett.*, **42**, 1346–1351, doi:10.1002/2014GL063015.

Usoskin, I. G., M. Korte, and G. A. Kovaltsov, 2008: Role of centennial geomagnetic changes in local atmospheric ionization. *Geophys. Res. Lett.*, **35**, L05811, doi:10.1029/2007GL033040.

Wu, Z., N. E. Huang, S. R. Long, and C. K. Peng, 2007: On the trend, detrending, and variability of nonlinear and non-stationary time series. *Proc. Natl. Acad. Sci. USA*, **104**, 14 889–14 894, doi:10.1073/pnas.0701020104.

——, ——, J. M. Wallace, B. V. Smoliak, and X. Chen, 2011: On the time-varying trend in global-mean surface temperature. *Climate Dyn.*, **37**, 759–773, doi:10.1007/s00382-011-1128-8.

Wyatt, M. G., and J. A. Curry, 2014: Role for Eurasian Arctic shelf sea ice in a secularly varying hemispheric climate signal during the 20th century. *Climate Dyn.*, **42**, 2763–2782, doi:10.1007/s00382-013-1950-2.

——, S. Kravtsov, and A. A. Tsonis, 2012: Atlantic multidecadal oscillation and Northern Hemisphere's climate variability. *Climate Dyn.*, **38**, 929–949, doi:10.1007/s00382-011-1071-8.

Yeager, S., and G. Danabasoglu, 2014: The origins of late-twentieth-century variations in the large-scale North Atlantic circulation. *J. Climate*, **27**, 3222–3247, doi:10.1175/JCLI-D-13-00125.1.

Zhou, Y. H., D. A. Salstein, and J. L. Chen, 2006: Revised atmospheric excitation function series related to Earth's variable rotation under consideration of surface topography. *J. Geophys. Res.*, **111**, D12108, doi:10.1029/2005JD006608.